

## 8.1 HPC for improved efficiency on standard machine tools by using new fluid-driven spindles

A. Schubert <sup>1</sup>, O. Harpaz <sup>2</sup>, B. Books <sup>2</sup>, U. Eckert <sup>1</sup>, R. Wertheim <sup>1</sup>
<sup>1</sup> Fraunhofer IWU, Reichenhainer Str. 88, 09126 Chemnitz, Germany

<sup>2</sup> Colibri Spindles Ltd., Lavon Industrial Park, M.P. Bikat Bet Hakerem 25127, Israel

### Abstract

The use of fluid-driven spindles is well known for machining various components, but not in real metal cutting. Machining of larger precision components as prototypes, tools and dies requires the use of relatively large machine tools and high-performance spindles. Usually these are mechanical spindles with relatively high power, displaying a rather low maximum speed of approximately 15,000 rpm. However, in semi-finishing and finishing with HPC conditions and in micro machining, the required rotation speeds are higher and the required power is lower.

This paper presents sustainability and efficiency using fluid-driven spindles for HPC on standard machine tools with small tool diameters and rotation speeds of up to 90,000 rpm using air and 30,000 rpm using the coolant flow. The fluid-driven spindle leads to a significant widening of the application range of larger machine tools and to an improvement of productivity by higher efficiency and faster tool- and spindle change, respectively.

### Keywords:

HPC; Cutting; Tools; Spindle

## 1 INTRODUCTION

Machining of large precision components for the dies and molds industry, for aerospace applications or for the machine tool industry requires the use of large machine tools with relatively high power spindles but with relatively low to medium rotation speeds of up to 15,000 rpm. A growing demand for micro structures, engravings, surface modifications or micro-functional geometries can be observed for many of the machined parts. On the one hand, using the heavy duty spindles for this range of applications is difficult and uneconomic due to the lower rotation speed and limited performance. On the other hand, using an additional micromachining center with small working area does not allow heavier parts and is uneconomic because of high investment cost, short productive time and lower efficiency.

The use of an additional fluid-driven spindle on the same heavy duty machine utilizes the standard air supply or the coolant supply system of the machine, improving efficiency, cost and saves additional machining equipment.

The current investigation presents the theoretical background, the properties of the fluid-driven spindles and the machining performance of the air and coolant-driven spindles.

## 2 COMPARISON OF ELECTRICAL, MECHANICAL AND FLUID-DRIVEN SPINDLES

Fig. 1 shows a comparison of various spindle types for rotation speed enhancement which can be used in combination with the machine tool main spindle. While the electrically and mechanically driven spindles require separate energy sources for the spindle and the coolant supply with or without using a speed increaser, the new unique fluid-driven

spindle is rotating and cooling the machining area with a single energy source. The new fluid-driven spindles can be mounted on the standard machine tool spindle with minimal setup time, can be gripped automatically in the tool changer and stored in the tool magazine. Flushing can be carried out for the various spindle concepts through the main spindle or externally.

The air-driven spindle can provide high rotational speed, tested here with up to 90,000 rpm and small torque and a coolant spindle with up to 30,000 rpm.

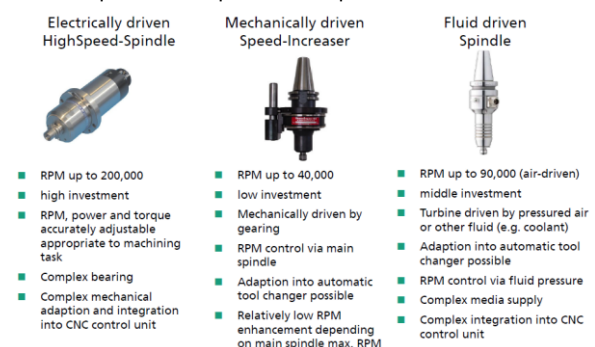


Figure 1: Comparison of spindle solutions for RPM enhancement which are adaptable in addition to the machine tool main spindle.

Fig.2 illustrates the cross section of the air- and the coolant-driven spindle concept (A) and (B), including a shank for clamping, a turbine for actuation, bearings, housing and the medium supply channels. The design enables the use of a wide range of replaceable tools clamped directly into the

spindle as well as the utilization of standard tool clamping devices.

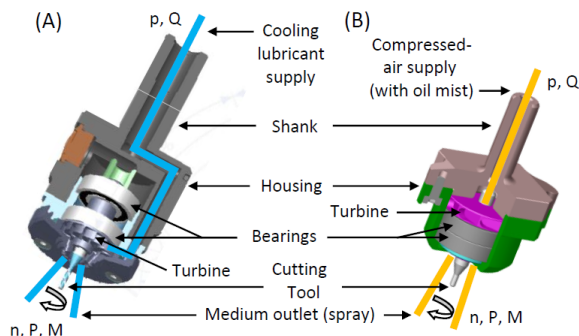


Figure 2: Cross section of the coolant-driven (A) and the air-driven (B) spindle concept.

In order to enable flexibility and to guarantee reliability and repeatability during machining with this spindle concept the design includes some unique features. The spindle shank can be clamped as a unit into any available standard main spindle device of the machine tool, or it can be mounted parallel to the main spindle. By selecting and controlling the air or coolant supply, especially as regards pressure ( $p$ ) and flow rate ( $Q$ ), it is possible to control or to achieve nearly constant rotation speed ( $n$ ), torque ( $M$ ) and power output ( $P$ ).

### 3 THE AIR-DRIVEN SPINDLE

The air-driven spindle (Fig. 2 B) offers high RPM of up to 90,000 min<sup>-1</sup>, but relatively low power output of less than 50W. Therefore, the actuation concept is only applicable for very small tool diameters and micromachining processes. Due to the limited torque, further finishing operations of high performance cutting with small tool diameters cannot be realized with the air-driven spindle concept. The following chapters 3.1 and 3.2 describe some fundamental investigations using the air-driven spindle concept.

#### 3.1 Air Pressure and Rotation Speed

The investigations of the air-driven spindles were carried out with various exchangeable heads, including integrated cutting tools:

- Two exchangeable heads with  $\varnothing$  of 0.5mm - Solid carbide end mills with 2 flutes and a helix of 30°. One of them with easily rotating spindle due to larger bearing clearance (approximately 40 $\mu$ m), and the other one nearly without bearing clearance (approximately 4 $\mu$ m)
- Two exchangeable heads with  $\varnothing$  of 1.0mm - Solid carbide short ball nose end mills with 2 flutes, helix of 30° and nearly without bearing clearance (approximately 4 $\mu$ m).

The rotation speed was checked in comparison with a spindle of a Kugler 5-axis machining center. A calibration test was realized with the fluid-driven spindle with an air pressure of 5.5 bar to prepare the RPM control unit for the repeatable rating tests of the new spindle. Further investigations were realized without real cutting to define the characteristics of the above described spindles with the various exchangeable heads. It could be detected that without machining a 7 bar air inlet pressure is required in order to reach 120,000 RPM. Fig. 3 presents the progression of rotation speed and air-flow rate

for the four exchangeable heads as a function of the air inlet pressure. It could be found that the flow rate behavior for all four tested tools as a function of the air pressure does not depend on the bearing clearance or on the tool diameter. It could also be shown that the run out is almost independent of the flow rate or air pressure.

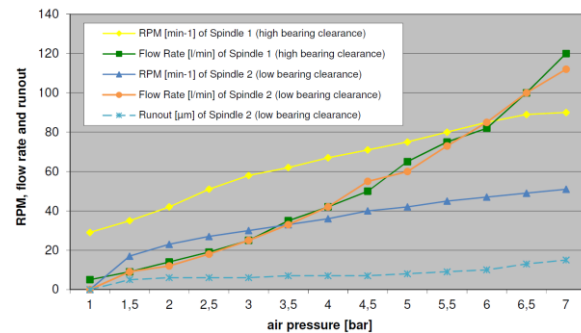


Figure 3: Rotation speed, flow rate and runout as a function of air inlet pressure and bearing clearance.

It can be concluded that an easy rotating spindle 1 with a clearance of 40 $\mu$ m can reach 90,000 RPM, while due to a smaller tolerance of 4 $\mu$ m and a higher resistance of spindle 2 the max. rotation speed is only 50,000 RPM. Therefore, an optimization process of the bearing design is required for optimal performance of the air-driven spindle.

#### 3.2 Machining Conditions and Performance

The cutting tests were carried out with a  $\varnothing$  of 0.5mm - Solid carbide end mills with 2 flutes and a helix angle of 30°. The rotation speed was 45,000 min<sup>-1</sup>, which is equivalent to  $v_c = 70$ m/min. The feed per tooth was 2 $\mu$ m, which is equivalent to a table speed of  $v_f = 180$ mm/min. The depth of cut  $a_p$  varied between 0.01mm and 0.4mm and the width of cut  $a_e$  varied between 0.005mm and 0.025mm.

The overview of the different geometrical machined shapes are shown in Fig. 4 (a to e). The selected finishing conditions are indicated below for each of the machined shapes.

a) Finishing a fin in down milling with  $a_p = 0.2$ mm and  $a_e = 0.025$ mm with overall 4 steps  $a_e$  and a total width of 0.1mm. High accuracy was achieved with relatively small tool deflection. Fin height was 198 $\mu$ m and width was 208 $\mu$ m. A good perpendicularity with a width difference of +8 $\mu$ m could be reached. The surface quality was evaluated using a confocal microscope and the surface quality results are at bottom  $R_z = 1.1\mu$ m and at flank  $R_z = 2.3\mu$ m.

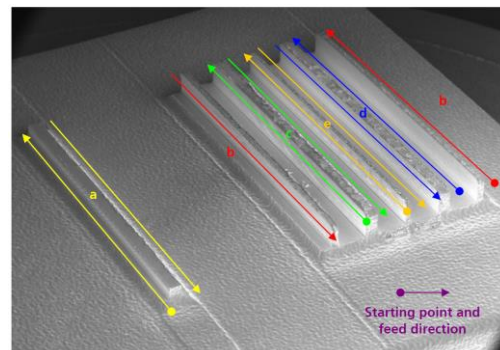


Fig. 4: Machining order of different geometrical shapes with different cutting conditions using the air-driven spindle.

b) Finishing a flank in up milling with a higher load of  $a_p = 0.4\text{mm}$  and  $a_e = 0.025\text{mm}$  with 5 steps of  $a_e$  overall and a total width of  $0.125\text{mm}$ . Good accuracy was reached with a measured deviation in width of  $-6\mu\text{m}$  compared to the targeted value. However, a small deflection of the fin was detected after the last cutting step no. 5, probably due to the increased cutting depth of  $0.4\text{mm}$ . The surface quality showed only a small deviation in comparison to the results in machining step a) with the smaller depth of cut  $a_p$ .

c) Roughing a fin from the solid in down milling with  $a_p = 0.01\text{mm}$  and  $a_e = 0.5\text{mm}$  with 40 steps of  $a_p$  overall and a total cutting depth of  $0.4\text{mm}$ . A comparatively good geometrical accuracy was achieved with a width deviation of  $+10\mu\text{m}$  and a height deviation of  $-12\mu\text{m}$  compared to the reference. The deviation in height could be explained by tool wear.

d) Roughing a fin from the solid in up milling with  $a_p = 0.01\text{mm}$  and  $a_e = 0.5\text{mm}$  with 40 steps of  $a_p$  overall and a total cutting depth of  $0.4\text{mm}$ . A comparatively good geometrical accuracy was achieved with a width deviation of  $+7\mu\text{m}$  and a height deviation of  $-15\mu\text{m}$  compared to reference. The increasing deviation in height could be explained by tool wear.

e) Finishing a  $0.4 \times 0.050\text{ mm}$  fin, shown in Fig. 5, in down milling with  $a_p = 0.4\text{mm}$  and  $a_e = 0.005\text{mm}$ , including a burr removal at zero level before finishing the flank with 5 steps of  $a_e$  overall and a total cutting width of  $0.025\text{mm}$ .

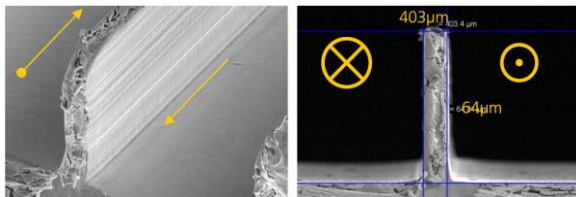


Fig. 5: SEM pictures of the finished fin (e) with the new air-driven spindle under finishing conditions.

Acceptable geometrical accuracy was achieved with a maximum width deviation of  $+14\mu\text{m}$  and a height deviation of  $+3\mu\text{m}$  compared to the nominal reference values.

### 3.3 Conclusion of Investigations of the Air-Driven Spindle

Good RPM-stability (after running-in) is achievable under constant air conditions (pressure, oil mist, flow rate). The use of a MQL system with medium flow rates is difficult to adjust. Consistently typical results for accuracy and surface quality could be achieved during the different machining operations. The tool wear was inconspicuous for the preliminary tests and no thermal effects were detectable during operating of the new air-driven spindle. The temperature of the spindle was nearly constant during the machining operations. Only some vibrations were detectable during cutting, but obviously without effecting surface quality.

It is very interesting and easy to use this spindle concept with limited power and torque, for example for parallel HSC-operations and micromachining processes. It has a high potential for use on conventional machine tools, depending on machine stability.

Detailed characteristics and operating behavior of the new air spindle concept have to be investigated, and it is required to check limits of the new spindle concept under various

influencing variables. In comparison to the air spindle, higher reliability and repeatability can be expected with the coolant-driven spindle.

## 4 THE COOLANT-DRIVEN SPINDLE

### 4.1 Basic Function of the Coolant-Driven Turbine Spindle and Spindle Modifications

During the investigations basic calculations were realized concerning design and dimensions of turbines. The layout and dimensions of both, the turbine blade geometry and the fluid inlet channels, were broadly investigated, calculated and optimized. The theoretical idle RPM, the torque and the power output for different fluid-driven turbine types and geometries were investigated as a function of rotation speed and coolant flow conditions. Analysis of the torque, the loss of RPM and the power output can define an efficiency factor. The results of the theoretical analysis were compared with the results of practical investigations using real fluid-driven turbines [4]. Fig. 6, for example, shows the characteristic behavior of a medium to high power fluid-driven turbine. The diagram describes the calculated deviation of power output and torque as a function of turbine rotation speed. The various graphs present the maximum theoretical power output of the turbine (blue line - A), the increasing losses of power output as a function of increasing turbine speed (red line - B), the resulting turbine power output available for the machining process (green line - C) and the decreasing torque (purple line - D) as a function of increasing turbine speed.

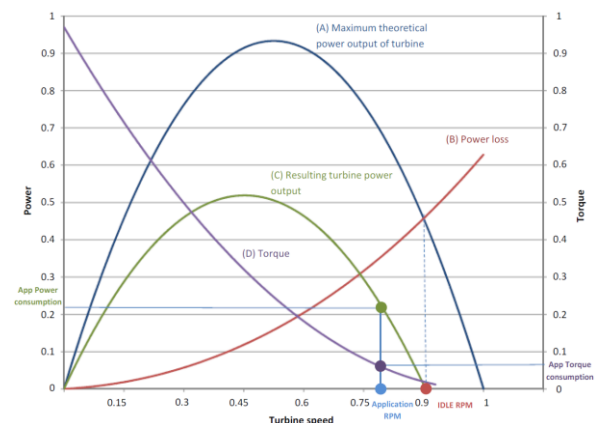


Fig. 6 Characteristic basic behavior of a typical fluid-driven spindle actuated by the cooling flow.

Fig. 6 illustrates that the fluid-driven turbine is limited as regards the available RPM range. In general, the recommended operating range is defined between 65% and 95% of the IDLE rotation speed. Lower speeds are not efficient while higher rotation speed reduces torque and power output significantly. The example indicated in the figure shows that for about 78% of the rotation speed the torque is less than 10% and the resulting power output for cutting is about 22% of the maximum value.

Literature offers similar range maps that describe different turbine types and allow selection of a turbine type and specifications according to the application requirements. The selection depends on fluid inlet pressure ( $p$ ), flow rate ( $Q$ ), power output ( $P$ ) and output rotation speed ( $n$ ). However, most of these publications refer to significantly larger turbines using higher power [4]. For lower power, as in our case, the



theoretical behavior and the experimental characteristics have to be investigated by using various design and geometrical features.

#### 4.2 Design and Features of the Fluid-Driven Spindle

During the investigation the turbine design including fan form, number of blades and fluid inlet/outlet geometry were optimized for maximum efficiency resulting in a unique structure. It was found that the designed and optimized small turbine shown in Fig. 7 (A) deviates far from the commonly accepted structures. Hence, only limited design criteria are known which can be used for the present application. The final fluid-driven spindle used in the investigation and shown in Fig. 7(B) and 7(C) is designed for a power output range of less than 1 kW.

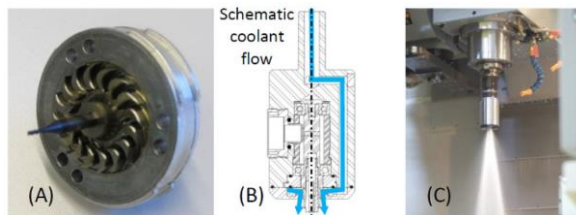


Fig. 7: The turbine fan design (A), cross section of the spindle (B) and the spindle actuated by the cooling lubricant (C)

First the general conditions were investigated for the application of the spindle concept on a machine tool. The concept of the spindle required a supply of cooling lubricant or pressured air through the clamping shank for operating the spindle. Therefore, different interfaces for reliable clamping of the spindle were analyzed. Collet chuck holders or shrink collets are possibilities for a spindle adaption with a standardized tool holder (e.g. HSK63-A). Fig. 8 presents, for example, the second spindle prototype in which the tool is clamped into a holder with shrink collet and also describes the main components of the spindle.

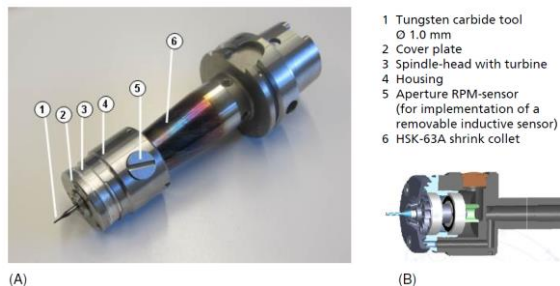


Fig. 8: Overview of the second spindle prototype mounted in holder (A) and cross section view (B).

#### 4.3 The Experimental Setup

Systematic and different investigation steps were carried out for analyzing and rating of the different prototypes of the spindle concept. This analysis mainly included the following points for a comprehensive rating of the spindle concept:

- Rotation speed (RPM) depending on coolant lubricant pressure (pump and spindle)
- Measurement and calculation of power output depending on RPM
- Measurement of cutting forces in comparison with results from other high precision spindles for micromachining

- Measurement of spindle stiffness
- Rating of achievable surface quality and geometrical accuracy
- Design optimization based on measuring results

For example, the evaluation of machining performance was carried out in real cutting tests based on the machining conditions. These tests featured various materials machined by various coated tungsten carbide tools. A special experimental setup was developed to measure the power output and to calculate the torque. Additional measuring methods such as measurements of the cutting forces were used to rate the machining characteristics and performance of the new spindle systems and to give further feedback concerning design and dimensions of the spindles (e.g. for dimensioning the bearings) [5]. A conventional method was tested using a torque measuring shaft device for measuring the values. This torque measuring shaft is problematic at higher RPM and disadvantageous during operations with high torque of inertia. Also the placement of the tested components is difficult without lateral off-set. These problematic facts require the development of a new and improved test setup (Fig. 9) for measuring torque and power output under various load conditions. This new setup is based on a generator (electric motor) which is driven by the spindle concept. The connection is realized with a balanced clutch. A sheet metal is used to avoid mechanical load on the bearings of the generator by high pressure coolant lubricant.

Before any measuring of torque and power output the detection of the characteristic power curve of the electric motor was required for envisaged use as a generator. Therefore the generator (electric motor) was driven by a second identical electric motor while the power input and output was measured with a power measuring device and the characteristic power curve was reproducibly documented. The identified characteristic power curve of the electric motor was basically used for further investigations and calculations for rating the spindle.

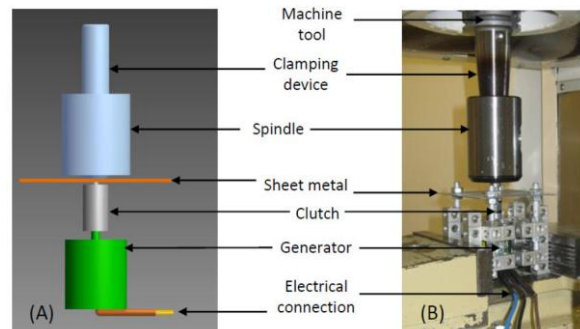


Fig. 9: Newly developed setup for measurement of power output (A) concept (B) implementation into machine tool.

#### 4.4 Features and Performance

In order to simulate different cutting conditions, the equipment was completed with a special setup to stress the spindle with various electrical loads. The following Fig. 10 presents the performance of the spindle concept measured with the load measurement setup. In this case, the power output is presented as a function of rotation speed and coolant pressure at pump.

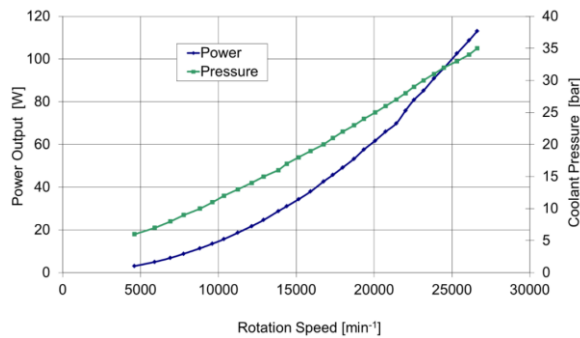


Fig. 10: Power output as a function of cooling lubricant pressure (at pump) and rotation speed for the selected spindle design.

In order to further rate the potential and the machining range different machining operations were realized while measuring the cutting forces with a 3-axis dynamometer. Investigations were first carried out on a micromachining center with a conventional HSC spindle and later repeated using the fluid-driven spindle concept to evaluate and compare the test results. Simple machining operations including slotting, shouldering and drilling of steel and aluminum were carried out and investigated using numerous different cutting parameters. A good correlation of the cutting forces could be determined between standard micromachining and machining with the fluid-driven spindle. The effective cutting forces are quite small and unproblematic for machining operations. The maximum forces could reach high values, so it is important to use an adapted machining strategy to avoid tool breakage or higher RPM loss, especially at the start of cut or in jump down applications. Results of cutting force measurement with the fluid-driven spindle are shown in Fig. 11. The diagram presents the maximum cutting forces as a function of feed rate.

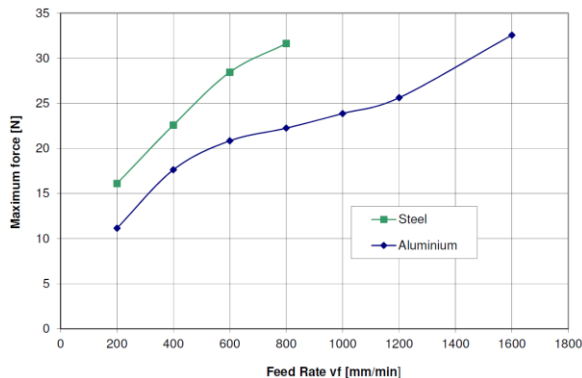


Fig. 11: Effective cutting forces as a function of feed rate in full slotting with  $\varnothing$  3mm tool.

The surface quality of the test samples was analyzed in machining steel and aluminum with different machining conditions. A confocal white light microscope (optical system) was used to rate the surface quality and to find a correlation to the used cutting parameters. A comparison of the surface quality with the values achieved using the conventional machining showed identical results. However, the use of the new spindle concept requires an adapted strategy and parameters because of some differences in spindle characteristics. The surface quality of steel is better than

aluminum. The depth of cut influences the surface quality in larger values due to deflection, while the lower quality in higher feed rates is expected due to larger tooth loads.

Another important rating criterion is the detection of the application range of the spindle concept. It indicates the limits for the achievable and useful range of rotation speed and corresponding to the machining power. Analyzing the machining process showed multiple factors for power losses: friction in the bearings, shaft misalignment as well as friction between the fluid and the rotating parts. Reducing power losses may result in significantly higher machining power, higher idle RPM and an improved efficiency factor. During the investigation the system was analyzed and modified to minimize friction and power losses, which are the main reason for the reduction of rotation speed of spindle under external load. It is important to calculate and define the minimum spindle speed and the cutting parameters in order to avoid overload on the cutting tool. High table feeds and larger depths of cut at low rotation speeds may result in high loads on the cutting edge and breakage. Fig. 12 illustrates the decrease of rotation speed as a function of cutting depth  $a_p$  when machining aluminum and steel.

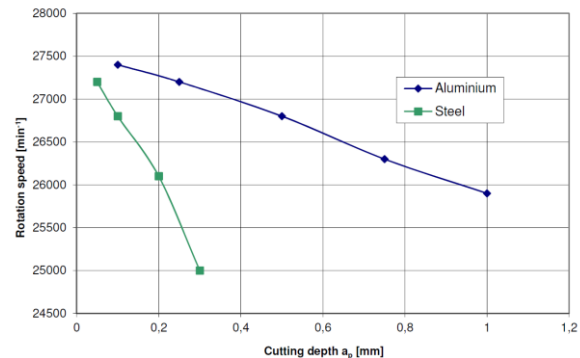


Fig. 12: Decrease of rotation speed as a function of cutting depth in milling aluminum and steel

All these investigation steps for rating the characteristics and performance of the spindle system provide important feedback to improve design, dimensions and machining behavior of the different prototypes [6].

#### 4.5 Machining Results

Machining tests were carried out on cold working steel 1.2379, using a standard tungsten carbide end mill with  $\varnothing$  1.0mm in face milling of an area of 50mm x 50mm. The tests were carried out at a cutting speed of 75m/min and feed rate of  $v_f = 300$  mm/min up to a removal volume of 125mm<sup>3</sup>. The final measured surface quality was very high, reaching  $R_z = 1.3\mu\text{m}$  and  $R_a = 0.2\mu\text{m}$ . Investigation results showing the microstructure and surface quality of a machined cold working steel 1.2379 are presented in Fig. 13.

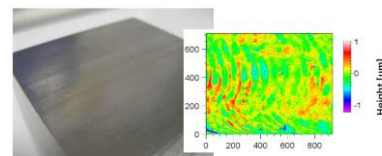


Fig. 13: Results of face milling in 1.2379.

Following these positive test results, further milling operations were carried out with various cutting parameters, e.g.

operations of slotting and shouldering of steel and aluminum. Machining of microstructure elements such as fins with a width of 50  $\mu\text{m}$  and a height-aspect ratio of 10 as shown for the air spindle can be carried out with high efficiency (Fig. 14). The geometrical and shape accuracy such as flatness (1.8  $\mu\text{m}$ ), parallelism (2.7  $\mu\text{m}$ ) or thickness and height are excellent and the surface finish was very good ( $R_z = 2.3 \mu\text{m}$ ), even at the bottom of the machined part, presented in table in Fig. 14 (B).

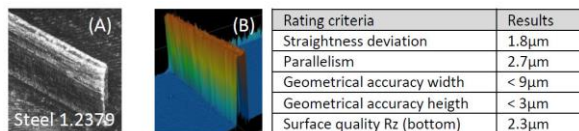


Fig. 14: Machined fin width 50  $\mu\text{m}$  and height 500  $\mu\text{m}$  (A), rating by 3D laser scanning microscope and results (B).

## 5 INDUSTRIAL APPLICATIONS

A machining example of a real component is shown in Fig. 14, using the fluid-driven spindle concept and the main machine spindle to demonstrate the technological potential of this solution. The machining parameters achievable with the new spindle compared with those of a conventional main spindle are presented in the table in Fig. 15. The new fluid-driven spindle reduces the machining time by 75% and improves the cost per workpiece, resulting in saving \$44 per part.

	Main spindle	Fluid-driven spindle
Tool diameter [mm]	1	1
Spindle speed [min <sup>-1</sup> ]	9,000	35,600
Cutting speed [m/min]	28	112
Feed per tooth [mm/tooth]	0.016	0.016
Table feed [mm/min]	288	1,140
Machining time per part [min]	60	13



Fig. 15: Machining results using the main machine spindle and the coolant-driven spindle for cutting a turbine made of stainless steel SAE 303 (1.4305).

Another case study describes the machining operations for roughing and finishing of an injection mold component using the fluid-driven spindle in comparison to the machine tool main spindle. During roughing the machining time could be reduced only by 18%, in comparison to roughing with the machine tool main spindle, higher cutting speeds allows for higher feed rates and optimized machining parameters in the finish milling process.

It could be impressively demonstrated that the use of the fluid-driven spindle improves the efficiency of the machining process by reducing machining time. Furthermore, the achievable surface quality while finishing under High Performance Cutting conditions can save an additional polishing process of the mold component.

## 6 SUMMARY

The test results with different prototypes of the spindle concept showed high performance of this new and innovative solution. It was demonstrated that the new concept is

functioning successfully when using the flushing system of the machine tool at a wide range of coolant inlet pressure (6-35bar). Moreover, it can be concluded that an integration of a control device for pressure and flow rate of the cooling lubricant can control the rotation speed (RPM) and power of the new spindle during operation.

A uniquely developed experimental setup made it possible to measure forces, power output and to calculate torque. Special measuring methods such as acoustic emission or measuring of cutting forces were used to rate the characteristics and performance of the spindle system and to give feedback concerning design and dimensions of the spindles.

The new and innovative spindle concept used in micromachining and finishing on conventional machine tools achieved high performance, good tool life and high surface quality. Furthermore, the new spindle concept improved efficiency and performance on CNC, on parallel kinematic machines and other machine tools, and reduced the cost of investment.

The project enabled to develop, to investigate and to define the machining conditions and performance of a complete new spindle concept.

More investigations should be carried out to explore the control of speed and fluid flow parameters. The efficiency and energy balance as well as saving of resources should be included in the next development step.

## 7 REFERENCES

- [1] Schubert, A., Schneider, J., Eckert, U.: Influence of special milling strategies on accuracy and surface quality of microstructured forms and prototypes. In: Proceedings of the 3rd International CIRP HPC Conference, Volume I-II, Dublin 2008, S. 131-140.
- [2] <http://www.eurekanetwork.org/project/-/id/5873>
- [3] Wertheim, R., Yitzhak, O.: SpinTool - the Spindle - Tool - System. Technical report at STC C meeting, 59th CIRP GA, Boston 8/2009.
- [4] Husain, Z., Abdullah, Z., Alimuddin, Z.: Basic Fluid Mechanics and Hydraulic Machines. CRC Press Taylor & Francis Group 2008
- [5] Harpaz, O., Books, B., Schwaar, M., Schubert, A., Eckert, U.: Parallel High Speed Machining with a New Additional HSC Spindle for Machine Tools. In: Proceedings of the 5th CIRP Conference on High Performance Cutting, Zurich 2012
- [6] Neugebauer, R., Drossel, W., Wertheim, R., Hochmuth, C., Dix, M.: Resources and Energy Efficiency in Machining Using High-Performance and Hybrid Processes. In: Proceedings of the 5th CIRP Conference on High Performance Cutting, Zurich 2012